IEEE Photonics Journal
An IEEE Photonics Society Publication

Open Access

A Tunable Single Passband Microwave Photonic Filter of Overcoming Fiber Dispersion Induced Amplitude Fading

Volume 9, Number 3, June 2017

Lu Xu
Xi Kong
Ziwei Wang
Haitao Tang
Xiaolong Liu
Yuan Yu, *Member, IEEE*
Jianji Dong, *Member, IEEE*
Xinliang Zhang, *Senior Member, IEEE*

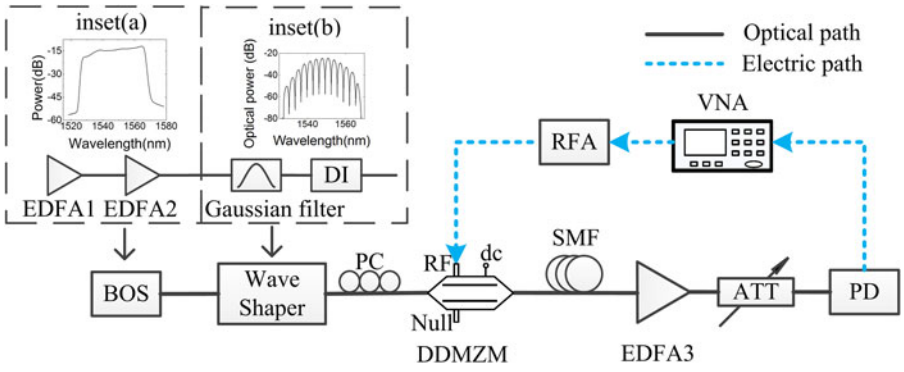

DOI: 10.1109/JPHOT.2017.2703940
1943-0655

IEEE photonics SOCIETY
IEEE

A Tunable Single Passband Microwave Photonic Filter of Overcoming Fiber Dispersion Induced Amplitude Fading

Lu Xu,[1] Xi Kong,[1] Ziwei Wang,[1] Haitao Tang,[1] Xiaolong Liu,[1] Yuan Yu,[2] *Member, IEEE*, Jianji Dong,[2] *Member, IEEE*, and Xinliang Zhang,[2] *Senior Member, IEEE*

[1]Wuhan National Laboratory for Optoelectronics, Huazhong University of Science and Technology, Wuhan 430074, China
[2]Wuhan National Laboratory for Optoelectronics and School of Optical and Electronic Information, Huazhong University of Science and Technology, Wuhan 430074, China

DOI:10.1109/JPHOT.2017.2703940

Manuscript received February 23, 2017; revised May 5, 2017; accepted May 9, 2017. Date of publication May 12, 2017; date of current version May 29, 2017. This work was supported in part by the National Natural Science Foundation of China under Grant 61501194, in part by the Hubei Provincial Natural Science Foundation of China under Grant 2015CFB231, in part by the Fundamental Research Funds for the Central Universities under Grant HUST: 2016YXMS025, and in part by the Director Fund of WNLO. Corresponding author: Y. Yu (e-mail: yuan_yu@hust.edu.cn).

Abstract: A tunable single passband microwave photonic filter (MPF) of overcoming fiber dispersion induced amplitude fading of the microwave passband is proposed and demonstrated. The passband amplitude of the MPF can be kept invariant for different central frequencies. The scheme is realized based on a dual-drive Mach–Zehnder modulator (DDMZM) and a broadband optical source sliced by a delay interferometer. The DDMZM is single-electrode driven and the microwave signal is modulated onto the optical carrier with simultaneous phase and intensity modulation formats. The ratio of the two modulation formats can be controlled by adjusting the bias of DDMZM to compensate the dispersion-induced amplitude fading at any passband of the MPF. In the experiment, the proposed MPF can be tuned between 0 and 30 GHz and the rejection ratio exceeds 30 dB.

Index Terms: Microwave photonic filter (MPF), microwave passband fading, dual-drive Mach-Zehnder modulator (MZM).

1. Introduction

Microwave photonic filters (MPFs) have been attracting great interests because of their inherent advantages which are superior to their electrical counterparts, such as low loss, large bandwidth, immunity to electromagnetic interference (EMI), excellent tunability and reconfigurability [1]–[3]. So far, many schemes have been proposed and successfully demonstrated based on various optical components [4]. However, the large tap delay introduced by optical fiber leads to small free spectral range (FSR) [5]–[8]. Therefore, most of these schemes exhibit multiple passbands in its operation bandwidth, which is disadvantageous for single band selection. In recent decades, extensive efforts have been directed to the design and implementation of different MPFs with single passband or stopband in order to effectively extract or suppressed the desired signals [9]–[14]. However, the passband shape in these schemes cannot be reconfigured to other filtering shapes because the tap coefficients cannot be changed, which limits the flexibility of the MPF. Meanwhile, the MPF with

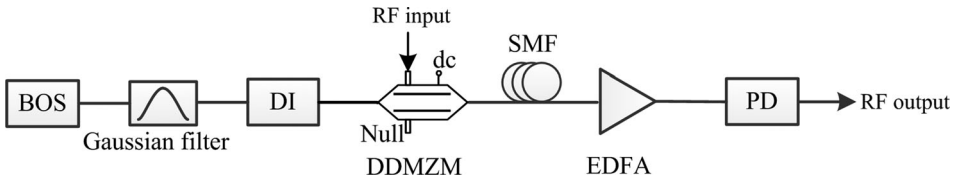

Fig. 1. Schematic diagram of the proposed filter. BOS: broadband optical source; DI: delay interferometer; DDMZM: dual-drive Mach-Zehnder modulator; SMF: single mode fiber; EDFA: erbium- doped fiber amplifier; PD: photodetector.

finite-impulse response (FIR) structure is also proposed with the advantage of excellent reconfigurability [15], [16]. More schemes of using broadband optical source and a fiber Mach-Zehnder interferometer (MZI) are proposed and successfully demonstrated [17], [18]. In this scheme, a span of optical fiber is used as the dispersive medium to introduce time delay. The MPF exhibits a single passband with large tunability. However, the chromatic dispersion of the optical fiber will lead to multi-band radio frequency (RF) power fading and deteriorate the amplitude response of the MPF [19]. Thus, more effort should be paid to overcome the amplitude fading of the MPF induced by fiber dispersion. A method of using a dual-input Mach-Zehnder electro-optic modulator can acquire a MPF with the dispersion-induced amplitude fading compensated [20]. Another method of using variable optical carrier time shift has been demonstrated to overcome the amplitude fading [21]. Due to the periodic changes of the modulation type between the intensity and phase modulations, the dispersion induced radio amplitude fading can be eliminated. However, the polarization state in one arm of the unbalanced MZI need to be adjusted accurately aligned with that in the other arm, which indicates that the stability may be deteriorated by environment fluctuation.

In this paper, we propose and demonstrate a single passband MPF based on a dual-drive Mach-Zehnder modulator (DDMZM) and a broadband optical source (BOS) sliced by a delay interferometer (DI) to overcome the dispersion induced amplitude fading. In the proposed MPF, the RF signal is applied to only one electrode of the DDMZM while the other one is left open. In this way, a complex modulation format contains both intensity modulation (IM) and phase modulation (PM) will be generated after DDMZM. The ratio of the two kinds of modulation format can be adjusted by changing the direct current (DC) bias of the modulator, which is different from those approaches that using MZI structure to alter the transmission characteristics of microring resonators by thermooptical or electrooptical method [22], [23]. Therefore, by employing the opposite microwave power fading induced by fiber dispersion between phase and intensity modulated signals, the microwave passband amplitude fading of the MPF induced by chromatic dispersion can be totally compensated. In experiment, the amplitude response at the passband of the MPF is successfully compensated over a frequency span of 0–30 GHz and the rejection ratio of the MPF exceeds 30 dB.

2. Operation Principle

The scheme of the proposed MPF is shown in Fig. 1. The complex electrical field of the BOS is expressed as

$$e(t) = \frac{1}{2\pi}\int_0^{+\infty} E(\Omega)\exp(j\Omega t)d\Omega. \tag{1}$$

The stochastic property of $E(\Omega)$ in (1) is given by [24]

$$\left\langle E(\Omega)E^*(\Omega')\right\rangle = 2\pi N(\Omega)\delta(\Omega-\Omega'), \tag{2}$$

where $N(\Omega)$ is the power spectral density and it describes the spectrum of BOS reshaped by a Gaussian profile optical filter and then spectrally sliced by the DI. $N(\Omega)$ is given by

$$N(\Omega) = \frac{P_0}{2\sqrt{\pi}} \frac{1}{\delta\Omega} \cdot \exp\left[-\left(\frac{\Omega - \Omega_0}{\delta\Omega}\right)^2\right]\left[1 + \exp\left(j2\pi \frac{\Omega - \Omega_0}{\Delta\Omega}\right)\right], \tag{3}$$

where P_0 is the total optical power emitted by the optical source, and $\delta\Omega$ is given by the full width at half maximum (FWHM) bandwidth $\delta\Omega_{3dB}$ in the form

$$\delta\Omega = \frac{\delta\Omega_{3dB}}{2\sqrt{\ln 2}}, \tag{4}$$

and $\Delta\Omega$ is the FSR of the DI.

The optical Gaussian filter is used to apodize the profile of the BOS and further makes the microwave passband of MPF exhibit Gaussian shape [25]. Then, the spectrally reshaped and sliced BOS is modulated by an input RF signal through the DDMZM.

Suppose that the input RF signal is $\cos(\omega_e t)$, where ω_e is the angular frequency of RF signal. Under small signal modulation, the modulated optical signal in the upper arm of DDMZM can be expressed as

$$E_1(\Omega) = \sqrt{P_1}\left[J_0 E(\Omega)\exp\left(j\frac{\pi}{2}\right) - J_{-1}E(\Omega - \omega_e) + J_1 E(\Omega + \omega_e)\right], \tag{5}$$

where P_1 is the power of optical carrier at the angular frequency of Ω, and J_n is the nth-order of the first kind Bessel function. It should be noted that $J_1 = -J_{-1}$. Therefore, (5) can be written as

$$E_1(\Omega) = \sqrt{P_1}\left[J_0 E(\Omega)\exp\left(j\frac{\pi}{2}\right) + J_1 E(\Omega - \omega_e) + J_1 E(\Omega + \omega_e)\right]. \tag{6}$$

As illustrated in Fig. 1, only the upper electrode of the DDMZM is driven by the RF signal while the other one is left open. Thus, a phase modulated signal can be generated in the upper arm of DDMZM. In this case, except for the optical carrier and $\pm$1st-order sidebands generated from the upper arm of DDMZM, a new pure carrier with adjustable phase shift is also generated in the lower arm. The optical carrier in the lower arm can be expressed as

$$E_2(\Omega) = \sqrt{P_1}E(\Omega)\exp(-j\theta), \tag{7}$$

where θ is the phase shift between the two arms of the DDMZM, which can be adjusted by changing the DC bias.

After modulation in the DDMZM, a span of single mode fiber (SMF) is used to provide time delay for different wavelengths. The dispersive device is modeled as an optical phase filter as

$$\Phi_d(\Omega) = \exp\left(-j\beta_2(\Omega - \Omega_0)^2/2\right), \tag{8}$$

where β_2 is the total dispersion and Ω_0 is the central frequency of the optical spectrum, respectively. Then the optical signal is fed into a photodetector (PD) and converted to the RF signal. By combining (1), (2), (6), (7) and (8), the electrical current generated by square-law detection of $E_1(\Omega)$ combined with $E_2(\Omega)$ after dispersion can be expressed as

$$\begin{aligned} I(\omega) &= \Re\left\langle \frac{1}{2\pi}\int_0^{+\infty} E_3(\Omega - \omega)d\Omega \right\rangle \\ &= 2\Re P_1 J_1\left[\delta(\omega - \omega_e) + \delta(\omega + \omega_e)\right] \\ &\quad \times \left\{ J_0 \int_0^{+\infty} N(\Omega)\cos\left(\frac{\pi}{2} + \frac{\beta_2\omega^2}{2}\right)\exp\left[-j\omega\beta_2(\Omega - \Omega_0)\right]d\Omega \right. \\ &\quad \left. + \int_0^{+\infty} N(\Omega)\cos\left(\theta + \frac{\beta_2\omega^2}{2}\right)\exp\left[-j\omega\beta_2(\Omega - \Omega_0)\right]d\Omega \right\}, \end{aligned} \tag{9}$$

where $E_3(\Omega) = [E_1(\Omega) + E_2(\Omega)]\Phi_d(\Omega)$ and $\Re$ is the responsivity of the PD. Since the DC component can only influence the response of the filter at zero Hertz which is not the main concern of our single passband MPF, and a strong DC component also affects the subsequent process of microwave signals. Thus, the DC component is usually blocked by alternating current (AC) coupling. Additionally, under small signal modulation, the second harmonic components are sufficiently small so its influence on the final response is negligible. Therefore, the DC and high order harmonic components are usually neglected [5], [26]. It should be noted that in frequency-domain the input microwave signal is $\pi[\delta(\omega - \omega_e) + \delta(\omega + \omega_e)]$. Thus the MPF's transfer function can be derived from (9)

$$H(\omega) = 4\Re P_1 J_1 \left[J_0 \cos\left(\frac{\pi}{2} + \frac{\beta_2 \omega^2}{2}\right) + \cos\left(\theta + \frac{\beta_2 \omega^2}{2}\right)\right] \times \left[H_b(\omega) + H_b\left(\omega - \frac{2\pi}{\beta_2 \Delta\Omega}\right)\right], \tag{10}$$

From (3), the baseband response $H_b(\omega)$ is defined by

$$H_b(\omega) = \frac{1}{2\pi} \int_0^{+\infty} \frac{P_0}{2\sqrt{\pi}} \frac{1}{\delta\Omega} \cdot \exp\left[-\left(\frac{\Omega - \Omega_0}{\delta\Omega}\right)^2 \right] \exp\left[-j\omega\beta_2 (\Omega - \Omega_0)\right] d\Omega. \tag{11}$$

It can be observed that (10) is composed of the baseband response and the bandpass response. From (10), it can be figured out that the central angular frequency of the microwave passband ω_0 satisfies

$$\omega_0 = 2\pi / \beta_2 \Delta\Omega. \tag{12}$$

Thus, it can be concluded that the central frequency of microwave passband can be changed by adjusting the FSR of DI. It can be noted that the chromatic dispersion in optical fiber is used to introduce time delay for different taps in this scheme. However, the fiber dispersion will lead to amplitude fading and deteriorate the amplitude response of the filter. It can be deduced from (10) that the amplitude response of the MPF $H_1(\omega)$ satisfies

$$H_1(\omega) \propto J_0 \cos\left(\pi/2 + \beta_2 \omega^2/2\right) + \cos\left(\theta + \beta_2 \omega^2/2\right). \tag{13}$$

From (13) we can see that $H_1(\omega)$ is composed of two parts. The first part alone on the right side of the equal sign is the dispersion induced amplitude fading, and when combined with the second part the amplitude fading can be totally compensated by adjusting the phase $\theta + \beta_2\omega^2/2$. By employing appropriate phase shift at different frequency, the fiber induced power fading can be compensated and the amplitude response of the MPF can be kept invariant for different central frequencies.

3. Experimental Results

The experimental setup of the proposed MPF is shown inFig. 2. The BOS is comprised of two cascaded EDFAs (Accelink EDFA-BA-16-FC/APC-2-3). The FWHM bandwidth of the amplified spontaneous emission (ASE) in EDFA1 is about 40 nm and the central wavelength is at 1547 nm, as shown in inset (a) of Fig. 2. The FWHM bandwidth and central wavelength of the optical spectrum after the waveshaper (Finisar WaveShaper 1000s) are about 40 nm and 1547.6 nm respectively, as shown in inset (b) of Fig. 2. Here the waveshaper works as a combined optical Gaussian bandpass filter and a DI so that the BOS will be reshaped by the optical Gaussian filter and spectrally sliced by the DI. The sliced BOS is then injected to a DDMZM (Fujitsu FTM7937EZ) and only one electrode is driven by the RF signal which is emitted from a vector network analyzer (VNA, Anritsu, MS4647B). Before applied to the DDMZM, the RF signal is amplified by a radio frequency amplifier (RFA, Centellax OA4SMM4). After transmission over a 10-km SMF with a total dispersion of $2.16 \times 10^{-22} s^2$(170 ps/nm), the optical signal is sent to a wideband PD (SHF AG Berlin) to be converted into an electrical signal, which is received by the VNA.

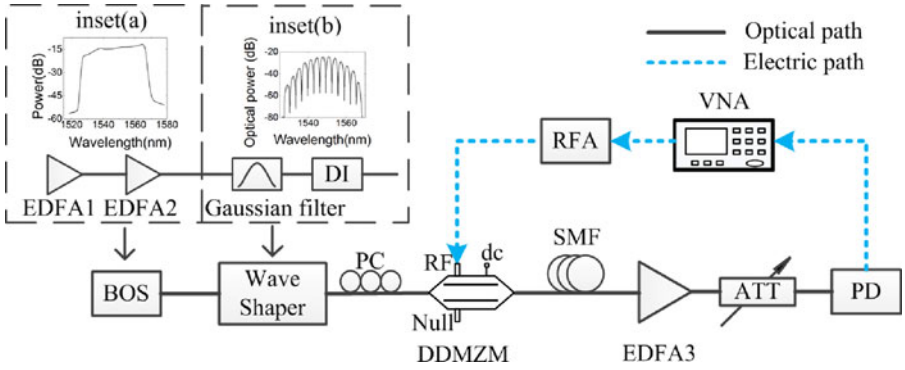

Fig. 2. Experimental setup of the proposed filter. BOS: broadband optical source; EDFA: erbium- doped fiber amplifier; DI: delay interferometer; PC: polarization controller; DDMZM: dual-drive Mach-Zehnder modulator; SMF: single mode fiber; ATT: attenuator; PD: photodetector; VNA: vector network analyzer; RFA: radio frequency amplifier.

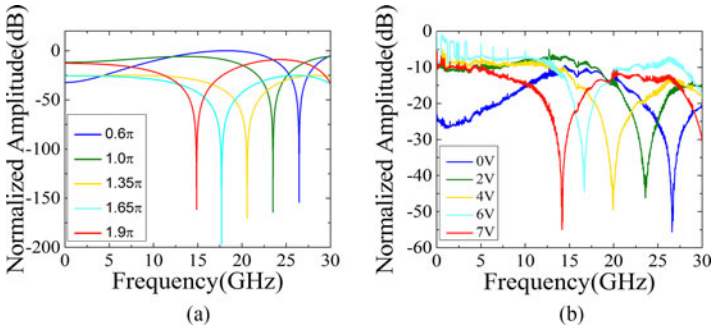

Fig. 3. The modulated signal transmission over a span of 10 km optical fiber with different phase shifts. (a) simulation results; (b) experiment results.

Based on (13), we simulated the modulated signal transmission over a span of 10 km optical fiber with different phase shifts while J_0 is approximated as 1, which is satisfied for small signal modulation. The simulation results are shown in Fig. 3(a). It can be observed that there is a notch in the frequency response from 0 to 30 GHz. When the phase shift between the two arms of DDMZM is changed from 0.6π to 1.9π, the notch could be shifted correspondingly. The experimental results are also shown in Fig. 3(b) for comparison. The phase shift in the lower arm of DDMZM is changed by tuning the DC bias of the DDMZM from 0 V to 7 V. It can be observed that the experimental results accord well with the simulation results.

The notch of the frequency response shown in Fig. 3 is also observed in Fig. 4(a) and (c) which show the simulation and experiment results of the proposed MPF with different central frequencies, respectively. Therefore, when no compensation is applied, the dispersion-induced power fading is distinctively observed, especially when the passband center is near 22 GHz where there is a notch in the single passband filter. In the simulation, which is based on (10), the total dispersion β_2 is set as $2.16 \times 10^{-22} s^2$,the bandwidth of the Gaussian filter is 30 THz and the phase shift is fixed at 1.17π firstly to simulate the occasion of no RF power compensation applied. The phase shift is also fixed in Fig. 4(c) by keeping the DC bias fixed at 5.4 V. The central frequency of the MPF is tuned by adjusting the FSR of DI as (12) shows. When the FSR of DI is set at 200 GHz, the measured frequency response of the MPF is shown as the purple curve in Fig. 4(c), and the measured optical spectrum after DI is shown in Fig. 5(a). It can be observed that the MPF is centered at 3.7 GHz. Then the FSR of DI is adjusted to tune the central frequency of the MPF from 4 GHz to 26 GHz with a 4-GHz step, as shown in Fig. 4(c). When the FSR of DI is set at 66.7 GHz, 40 GHz and 28.6 GHz, the measured amplitude response of the MPF are shown as the green curve, cyan curve and blue curve in Fig. 4(c) respectively, and the corresponding optical spectra after DI are shown in Fig. 5(b),

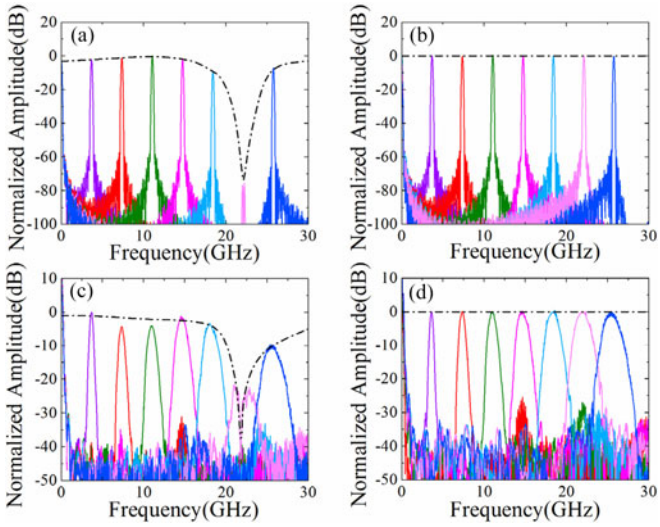

Fig. 4. Amplitude responses of the proposed MPF. (a), (b) are simulation results and (c), (d) are experiment results. The phase shift keeps fixed in (a), (c) and changes as the passband central frequency changes in (b), (d).

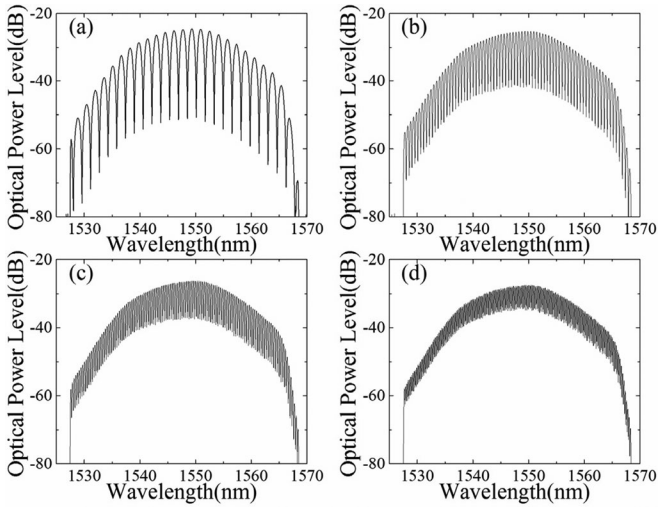

Fig. 5. The optical spectra after the DIs when the FSR of DI is (a) 200 GHz, (b) 66.7 GHz, (c) 40 GHz, and (d) 28.6 GHz.

(c) and (d) respectively. Because of the DDMZM bandwidth limitation, the tuning range of our MPF is restricted within no more than 30 GHz. If a DDMZM with larger bandwidth is used, the tuning range of the MPF will be broadened as well.

To compensate the dispersion induced RF amplitude fading, the phase shift θ needs to be adjusted as the central frequency of the MPF varies. When the phase shift θ changes, the transfer function expressed by (13) will change as well and the position of the notch will be shifted. By shifting the notch away from the passband of the MPF, the power fading at the central frequency of the microwave passband is compensated. By employing appropriate phase shifts at different passbands, the fiber induced power fading at any working frequency can be compensated and the passband amplitude of the MPF can be kept invariant for different central frequencies. It should be noted that during the experiment, the phase shift is changed by tuning the DC bias of the DDMZM while in simulation we can change the phase shift directly. The specific operation parameters of both the simulation and the experiment are listed inTable 1. With the compensation applied, the

TABLE 1
Specific Parameters of Simulation and Experiment Results

FSR of DI (GHz)	Simulation parameters		Experiment parameters	
	Central frequency of MPF (GHz)	Phase shifts (π)	Central frequency of MPF (GHz)	DC bias of DDMZM (V)
200	3.67	1.08	3.63	8.97
100	7.39	1.15	7.37	9.52
66.7	11.06	1.16	11.00	8.98
50	14.73	0.27	14.65	8.52
40	18.40	1.04	18.43	7.72
33.3	22.12	0.80	22.30	6.72
28.6	25.73	0.36	25.40	6.52

simulation and experiment results of the amplitude responses of the proposed MPF are shown in Fig. 4(b) and (d), respectively. It can be observed that the amplitude of the MPF keeps nearly constant when the frequency is tuned. Thus a tunable single passband MPF of overcoming fiber dispersion induced power fading is realized.

It can be noted that the FWHM bandwidth of the filter is broadened as the central frequency of passband increases. This is caused by third-order dispersion [27]. By properly setting the phase response of the programmable optical filter, the bandwidth of the MPF can be kept invariant [28].

4. Conclusions

A tunable single passband MPF of overcoming the dispersion induced amplitude fading of microwave passband has been proposed and successfully demonstrated. The scheme is realized by using a DDMZM and a broadband optical source sliced by a DI. The passband of the MPF can be tuned by adjusting the FSR of DI. In the proposed scheme, only one electrode of the DDMZM is driven by RF signals, while the other one is left open. By adjusting the DC bias of the DDMZM, the dispersion-induced amplitude fading at any passband can be totally compensated. In the experiment, the passband amplitude of the MPF can be kept nearly invariant when the passband is tuned from 0 to 30 GHz.

References

[1] A. J. Seeds, "Microwave photonics," *IEEE Trans. Microw. Theory Tech.*, vol. 50, no. 3, pp. 877–887, Mar. 2002.
[2] R. A. Minasian, "Photonic signal processing of microwave signals," *IEEE Trans. Microw. Theory Tech.*, vol. 54, no. 2, pp. 832–846, Feb. 2006.
[3] J. Yao, "Microwave photonics," *J. Lightw. Technol.*, vol. 27, no. 3, pp. 314–335, Feb. 2009.
[4] J. Capmany, B. Ortega, D. Pastor, and S. Sales, "Discrete-time optical processing of microwave signals," *J. Lightw. Technol.*, vol. 23, no. 2, pp. 702–723, Feb. 2005.
[5] Y. Yu, E. Xu, J. Dong, L. Zhou, X. Li, and X. Zhang, "Switchable microwave photonic filter between high Q bandpass filter and notch filter with flat passband based on phase modulation," *Opt. Express*, vol. 18, no. 24, pp. 25271–25282, Nov. 2010.
[6] E. Xu, F. Wang, L. Li, Y. Yu, X. Zhang, and D. Huang, "Cascaded microwave photonic filters with multiple infinite impulse responses based on wavelength conversion," in *Proc. Commun. Photon. Conf. Exhib.*, 2011, pp. 1–6.

[7] N. You and R. A. Minasian, "A novel high-Q optical microwave processor using hybrid delay-line filters," *IEEE Trans. Microw. Theory Tech.*, vol. 47, no. 7, pp. 1304–1308, Jul. 1999.
[8] K. K. Loh, K. S. Yeo, Y. G. Shee, F. R. M. Adikan, and M. A. Mahdi, "Microwave photonic filter using multiwavelength Brillouin-erbium fiber laser," *IEEE Photon. Technol. Lett.*, vol. 27, no. 1, pp. 65–68, Jan. 2015.
[9] Y. M. Chang and J. H. Lee, "High-Q, tunable, photonic microwave single passband filter based on stimulated Brillouin scattering and fiber Bragg grating filtering," *Opt. Commun.*, vol. 281, no. 20, pp. 5146–5150, Jun. 2008.
[10] W. Li, M. Li, and J. Yao, "A narrow-passband and frequency-tunable microwave photonic filter based on phase-modulation to intensity-modulation conversion using a phase-shifted fiber Bragg grating," *IEEE Trans. Microw. Theory Tech.*, vol. 60, no. 5, pp. 1287–1296, May 2012.
[11] N. Ehteshami, W. Zhang, and J. Yao, "Optically tunable single passband microwave photonic filter based on phase-modulation to intensity-modulation conversion in a silicon-on-insulator microring resonator," in *Proc. Int. Topical Meeting Microw. Photon.*, 2015, pp. 1–4.
[12] D. Marpaung *et al.*, "Si3N4 ring resonator-based microwave photonic notch filter with an ultrahigh peak rejection," *Opt. Express*, vol. 21, no. 20, pp. 23286–23294, Oct. 2013.
[13] X. Han and J. Yao, "Bandstop-to-bandpass microwave photonic filter using a phase-shifted fiber Bragg grating," *J. Lightw. Technol.*, vol. 33, no. 24, pp. 5133–5139, Dec. 2015.
[14] W. Zhang and R. A. Minasian, "Switchable and tunable microwave photonic Brillouin-based filter," *IEEE Photon. J.*, vol. 4, no. 5, pp. 1443–1455, Oct. 2012.
[15] M. Song, C. M. Long, R. Wu, D. Seo, D. E. Leaird, and A. M. Weiner, "Reconfigurable and tunable flat-top microwave photonic filters utilizing optical frequency combs," *IEEE Photon. Technol. Lett.*, vol. 23, no. 21, pp. 1618–1620, Nov. 2011.
[16] Y. Yu, S. Li, X. Zheng, H. Zhang, and B. Zhou, "Tunable microwave photonic notch filter based on sliced broadband optical source," *Opt. Express*, vol. 23, no. 19, pp. 24308–24316, Sep. 2015.
[17] K. Zhu, H. Ou, H. Fu, E. Remb, and S. He, "A simple and tunable single-bandpass microwave photonic filter of adjustable shape," *IEEE Photon. Technol. Lett.*, vol. 20, no. 23, pp. 1917–1919, Dec. 2008.
[18] J. Mora *et al.*, "A single bandpass tunable photonic transversal filter based on a broadband optical source and a Mach-Zehnder interferometer," in *Proc. Int. Topical Meeting Microw. Photon.*, 2003, pp. 251–254.
[19] J. L. Corral, J. Marti, and J. M. Fuster, "General expressions for IM/DD dispersive analog optical links with external modulation or optical up-conversion in a Mach-Zehnder electrooptical modulator," *IEEE Trans. Microw. Theory Tech.*, vol. 49, no. 10, pp. 1968–1976, Oct. 2001.
[20] L. Li, X. Yi, T. X. Huang, and R. A. Minasian, "Shifted dispersion-induced radio-frequency fading in microwave photonic filters using a dual-input Mach–Zehnder electro-optic modulator," *Opt. Lett.*, vol. 38, no. 7, pp. 1164–1166, Apr. 2013.
[21] X. Xue, X. Zheng, H. Zhang, and B. Zhou, "Widely tunable single-bandpass microwave photonic filter employing a non-sliced broadband optical source," *Opt. Express*, vol. 19, no. 19, pp. 18423–18429, Sep. 2011.
[22] X. Zhang, T. Zhang, X. Xue, Y. Cui, and P. Wu, "Resonant frequency shift characteristic of integrated optical ring resonators with tunable couplers," *J. Opt. A: Pure Appl. Opt.*, vol. 11, no. 8, Jul. 2009, Art. no. 085411.
[23] X. Zhang *et al.*, "Tunable optical ring resonator integrated with asymmetric Mach–Zehnder interferometer," *J. Lightw. Technol.*, vol. 28, no. 17, pp. 2512–2520, Sep. 2010.
[24] D. Guang-Hua and E. Georgiev, "Non-white photodetection noise at the output of an optical amplifier: Theory and experiment," *IEEE J. Quantum Electron.*, vol. 37, no. 8, pp. 1008–1014, Aug. 2001.
[25] J. Ge and M. P. Fok, "Frequency band selectable microwave photonic multiband bandpass filter based on Lyot filter," in *Proc. 2015 Conf. Lasers Electro-Opt.*, 2015, Paper STh3F. 2.
[26] F. Zeng and J. Yao, "Investigation of phase-modulator-based all-optical bandpass microwave filter," *J. Lightw. Technol.*, vol. 23, no. 4, pp. 1721–1728, Apr. 2005.
[27] J. Mora *et al.*, "Photonic microwave tunable single-bandpass filter based on a Mach-Zehnder interferometer," *J. Lightw. Technol.*, vol. 24, no. 7, pp. 2500–2509, Jul. 2006.
[28] D. Zou, X. Zheng, S. Li, H. Zhang, and B. Zhou, "Idler-free microwave photonic mixer integrated with a widely tunable and highly selective microwave photonic filter," *Opt. Lett.*, vol. 39, no. 13, pp. 3954–3957, Jul. 2014.